Structural, morphological and optical characterization of chemically deposited Cu_2O/PbS thin films

R. O. Okoro[a], C. Augustine[b, c*], R. A. Chikwenze[b], S. O. Amadi[b], P. E. Okpani[d], E. P. Obot[b], B. J. Robert[e], , C. N. Ukwu[b], P. N. Kalu[b], C. O. Dike[b], K.O. Achilike[f], D. I. Oyor[g]

[a]*Department of Physics, Ebonyi State College of Education, Ebonyi State, Nigeria*
[b]*Department of Physics, Alex Ekwueme Federal University Ndufu-Alike, Ikwo, Nigeria*
[c]*Department of Industrial Physics, King David University of Medical Sciences, Uburu, Nigeria*
[d]*Department of Electrical and Electronic Engineering, Alex Ekwueme Federal University Ndufu-Alike, Ikwo, Nigeria*
[e]*Department of Electrical/Electronic Engineering Technology, Akanu Ibiam Federal Polytechnic, Unwana, Ebonyi State, Nigeria*
[f]*Department of Industrial Physics, Abia State University,Uturu, Nigeria*
[g]*Department of Science Laboratory Technology, Akanu Ibiam Federal Polytechnic, Unwana, Ebonyi State, Nigeria*

Cu_2O/PbS core-shell thin films were synthesized by a chemical bath deposition technique using a reactive mixture containing copper nitrate, lead nitrate, ethylenediaminetetraacetic acid, tetraethyl amine and ammonia solution. Their structural and optical properties are reported in this work. For the elemental composition estimation, Rutherford backscattering spectroscopy (RBS) was performed. From the proton induced scan on the substrate containing the films, all the elements that make up the films were extracted as Cu (34.86%), Pb (1.69%), S (42.31%) and O (65.15%). This is an indication that Cu_2O-PbS quaternary thin films were actually deposited on the substrate. The X-ray diffraction analysis showed the formation of multiple peaks indicating that the films possess polycrystalline structure. The scanning electron micrographs of the films depicted particles of different sizes scattered across the film surface. The absorbance, transmittance, absorption coefficient, band gap and extinction coefficient were modified by thermal annealing. Absorbance varies from 1.175 to 1.35 for as-grown, 1.475 to 1.50 for annealed at 150 ^oC and 1.65 to 2.00 for annealed at 200 ^oC. The percentage transmittance of 6.75 % was obtained for as-grown sample while those of the annealed samples are 6.0 % and 5.0 % at 150 ^oC and 200 ^oC respectively. Maximum absorption coefficient values are 3.48 x 10^6 m^{-1}, 3.68 x 10^6 m^{-1} and 4.60 x 10^6 m^{-1} for As-grown, annealed at 150 ^oC and 200 ^oC respectively. The band gap energy value is found to increase from 3.50 eV to 4.00 eV as a result of the increase in annealing temperature from 150 ^oC – 200 ^oC. Extinction coefficient values generally varies from 0.75 to 2.70 for as-grown, 0.80 to 2.85 for annealed at 150^oC and 0.85 to 3.00 for annealed at 200^oC. Based on the wide band gap exhibited by the films, it can be concluded that the films are suitable as window materials in the fabrication of solar cell devices.

(Received September 9, 2021; Accepted February 7, 2022)

Keywords: Band gap, Chemical bath, Annealing, Films, Transmittance

1. Introduction

Solar energy is a source of free, natural and non-polluting energy that man can harness for useful applications [1]. Thin films have been found important for various solar energy devices

* Corresponding author: emmyaustine2003@yahoo.com
https://doi.org/10.15251/CL.2022.192.93

such as mirror filters, anti-reflection coating photosynthetic coating, thermal and solar control coatings [2, 3]. Some are moderately selective while others are non-selective. Those films whose optical properties such as absorbance, transmittance, emittance, reflectance, etc. are dependent on wavelength are said to be spectrally selective films. For such films, the optical or radiative properties vary quantitatively with different parts of the electromagnetic spectrum [1].

In advanced countries, highly technological and very expensive thin films deposition techniques for optical, electronic and optoelectronic device application has become an industry. However, this is not so in third world countries due to the poverty of the third world countries. Hence, considerable efforts are put into developing simple and cheap techniques of depositing the films. The chemical bath deposition technique offers the simplest, cheapest, most economical and affordable method of depositing thin films like halides and chalcogenides.

The survey of literature showed that the solution growth technique has been extensively employed in the deposition of different binary thin films [1, 4-10] and ternary thin films [11-20]. However, the use of this technique for the deposition of quaternary thin films is limited. Few reports on the use of the chemical bath deposition technique for the deposition of quaternary thin films are available in the following references in the literature [21-29].

In this work, preparation of Cu_2O/PbS quaternary thin films using chemical bath deposition technique was described. These films are semiconductor compounds composed of four elements. The structural and optical properties of these films were analyzed.

2. Materials and methods

First, Cu_2O films were deposited from chemical bath comprising 15 mls of 0.3M of Cu $(NO_3)_2.3H_2O$, 15 mls of 0.05 M hydrazine (NH_2NH_2) , 5.3mls of 1M TEA and 9 mls of distilled water with P^H of 6.0 at 45 ^oC bath temperature for 2 hours. To achieve the deposition of Cu_2O/PbS quaternary thin films, the glass substrates containing Cu_2O film deposits were inserted into a chemical bath comprising 5 mls of 0.1M of Pb $(NO_3)_2$, 5mls of 0.1M of $(NH_2)_2CS$, 5 mls of 0.01M EDTA, 0.5 mls of 10M NH_3 solution and 34 mls of distilled water in that order with pH of 4.3 at bath temperature of 60 ^oC for 1 hour. Rutherford backscattering (RBS) was used to determine the elemental compositions, depth profile and thicknesses of the films by Proton Induced X-ray Emission (PIXE) scans on the samples from a Tandem Accelerator Model 55DH 1.7MV Pellaton The crystal structure and phase analysis of the deposited films were carried out at room temperature with an X-ray diffractrometer Rigaku Ultima IV model, using gracing incident at 30 mA, 40KV with CuKα radiation of wavelength λ = 0.15406nm selected by a diffracted beam monochromator. The thin films were scanned continuously between 0^o to 90^o at a step size of 0.034 and at a time per step of 56.7s. The XRD diffractograms of intensity versus 2θ values were generated and displayed. Phase identification was then made from an analysis of intensity of peaks versus 2θ, using ICDD data. Scanning electron microscope (SEM) was used for morphological studies. Thermo scientific GENESYS 10S model UV-VIS spectrophotometer was used to determine the absorbance of the deposited films in the wavelength range of 300-1000 nm

3. Result and discussion

Fig.1 depicts the quantitative measurement of elemental composition of the films. A glance on the figure indicated that all the elements that make up the films are present. The percentage composition of the films is shown in Table 1.

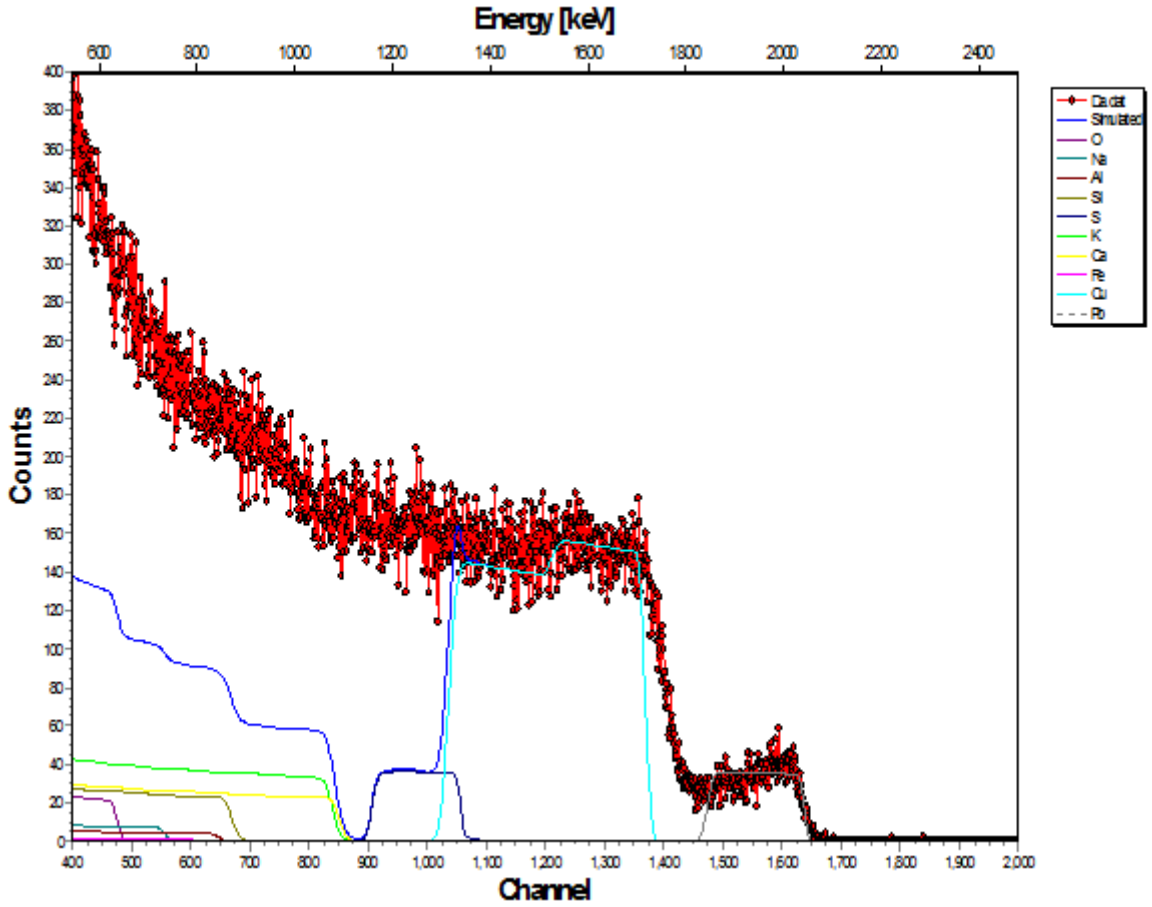

Fig. 1. RBS micrograph of Cu_2O/PbS quaternary thin films.

Table 1. % Composition of Cu_2O-PbS Quaternary Thin Films.

Elements	Glass substrate	Cu_2O-PbS Thin Film
Na	25.00	-
Ca	6.00	-
K	3.50	-
Al	5.20	-
Pb	-	1.69
Cu	-	34.86
S	-	42.31
Fe	0.30	-
O	26.00	65.15
Si	34.00	-

The XRD patterns of the films is presented in Fig. 2. The diffractograms of Cu_2O phase are characterized by peaks of 35.3°, 46.2° and 53.4° with JCPDS 44-0706 while those of PbS phase are characterized by multiple peaks of 26°, 30° and 52° with JCPDS card 00-05-0592. The multiple peaks observed in the XRD patterns of the films suggest that the films are polycrystalline. Similar verdict have been made by other authors [21, 22, 29].

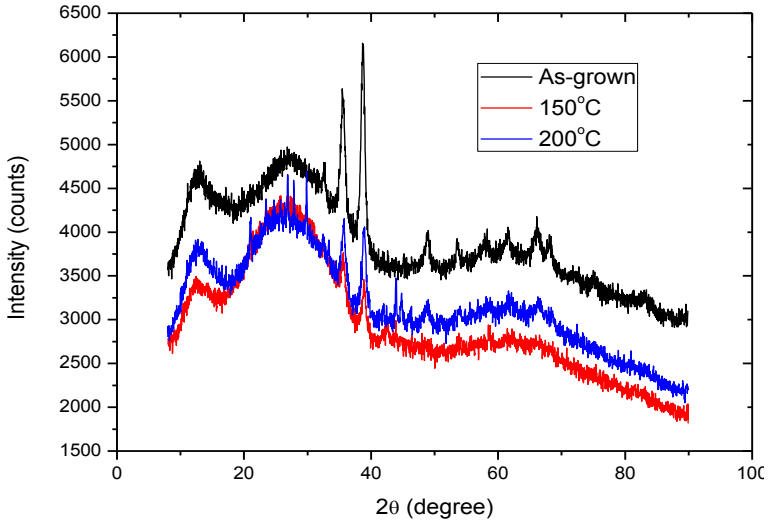

Fig. 2. XRD patterns of Cu_2O/PbS thin films.

All the SEM images are characterized by large particles scattered across the film surface (Fig 3-5). The SEM image of the film annealed at 150°C, showed a continuous and homogeneous distribution of grains on the substrates compared to other film samples.

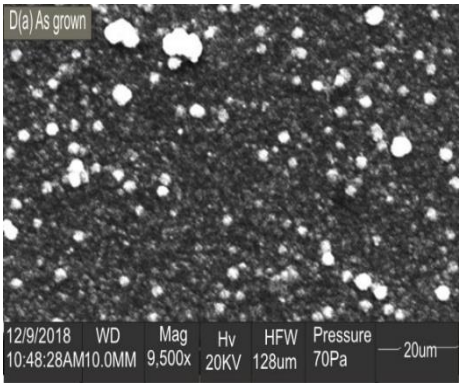

Fig. 3. SEM images of Cu_2O/PbS thin films for as-grown.

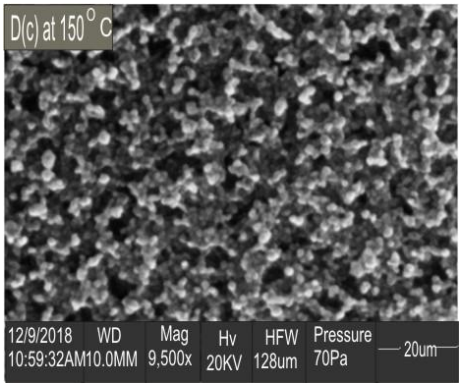

Fig. 4. SEM images of Cu_2O/PbS thin films for annealed at 150°C.

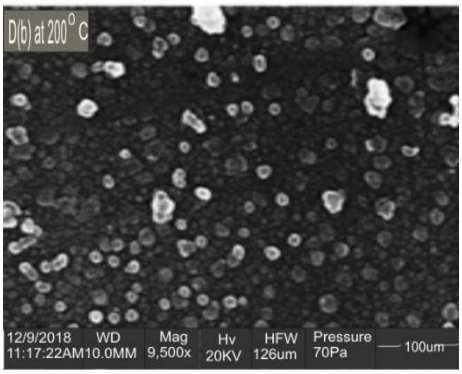

Fig. 5. SEM images of Cu_2O/PbS thin films for annealed at 200^oC.

It can be seen that the absorbance decreases as wavelength increases to 350 nm and then increases within 350-1000 nm (Fig. 6). All samples have good absorption of light in the infrared region. Absorbance varies from 1.175 to 1.35 for as-grown, 1.475 to 1.50 for annealed at 150 ^oC and 1.65 to 2.00 for annealed at 200 ^oC. In all these samples, the maximum absorbance shifts to the longer wavelength region for as-grown, annealed at 150 ^oC and to shorter wavelength for annealed at 200 ^oC. Our values of absorbance are in the same order of magnitude with values given by Agbo and Nnabuchi (2011) for TiO_2-ZnO core-shell thin films [15], Agbo *et al.* (2011) for TiO_2-Fe_2O_3 core-shell thin films [13] and Agbo *et al.* (2013) for TiO_2-CuO core-shell thin films [16]. However, Augustine and Nnabuchi (2018) [23] reported absorbance values that spans from 0.25 to 4.00 for CuO-PbS thin films deposited by chemical bath deposition technique, which is higher that our values of 1.175-2.00 for Cu_2O-PbS thin films deposited in this work. The concentration of reagents used may have accounted for the absorbance differentials. Absorbance and concentration are directly related according to Lambert-Beer's law.

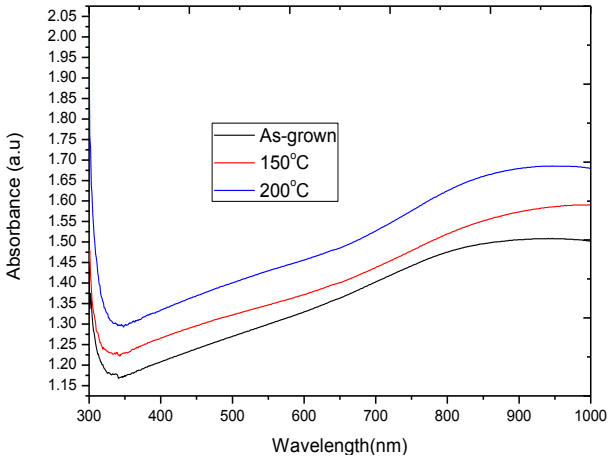

Fig. 6. Plot of absorbance against wavelength.

The transmittance of films is high for shorter wavelength and lower for longer wavelength (Fig. 7). Peak transmittance for all film samples occur at 350 nm. As-grown sample has maximum transmittance of 6.75 % while those of the annealed samples are 6.0 % and 5.0 % for annealed at 150 ^oC and 200 ^oC respectively. The maximum transmittance values are far lower compared to maximum of 25 %, 35 % and 50% for As-grown, annealed at 150 ^oC and 200 ^oC respectively reported by Augustine and Nnabuchi (2018) for CuO-PbS thin films deposited by chemical bath method [23]. The low transmittance is not unconnected with the high absorbance of the films. High absorbance suggest that more photons will absorb more light and transmit less light.

However, the maximum transmittance of 6.75 % reported in this work is in close agreement with maximum of 7 % by Augustine and Nnabuchi (2017) for PbS-NiO-CdO thin films [25].

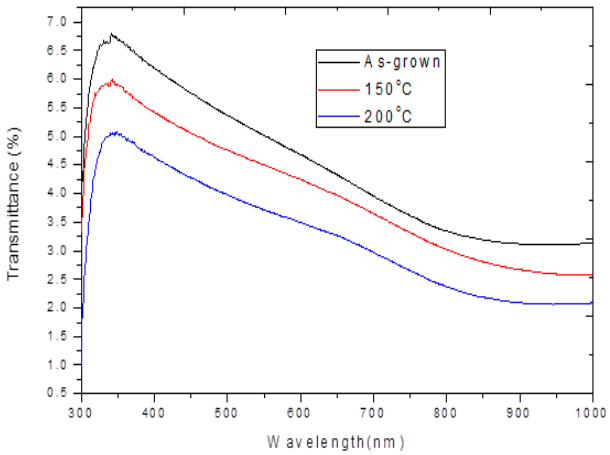

Fig. 7. Plot of Transmittance against wavelength.

It is observed that the reflective behaviour of films tends to reduce with increasing wavelength (Fig. 8). The reflectance spectra of films can be separated into two regions. In the first area up to 350 nm, there is a peak at about 330 nm corresponding to decrease in absorption and increasing transmission. In second area up to 1000 nm, there is minimum spectral reflectance corresponding to increasing absorption and decreasing transmission.

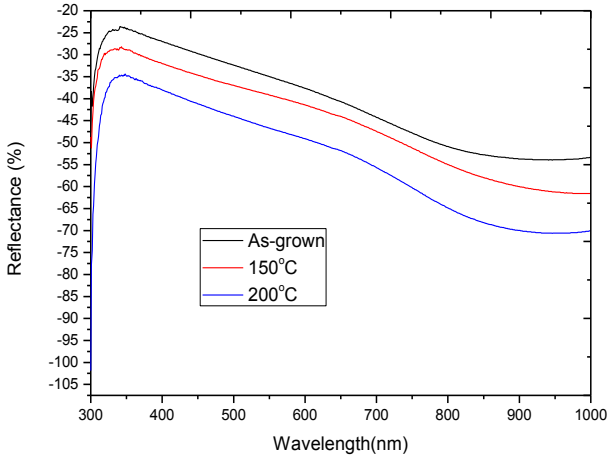

Fig. 8. Plot of reflectance against wavelength.

The absorption coefficient (α) decreases with photon energy up to 3.65eV and then increases within 3.75-4.13 eV (Fig. 9). Minimum α values are $2.7x10^6m^{-1}$, $2.8x10^6m^{-1}$ and $3.2x10^6m^{-1}$ for as-grown, annealed at 150°C and 200°C respectively while the maximum values are $3.48x10^6$ m^{-1}, $3.68x10^6$ m^{-1} and $4.60x10^6$ m^{-1} for As-grown, annealed at 150 °C and 200 °C respectively. These absorption spectra, which are the most direct and perhaps the simplest method for probing the band structure of semiconductors, are employed in the determination of the energy band gap, E_g. The photon energy at the point where $(\alpha h\nu)^2$ is zero represents E_g, which is determined by extrapolation. From Fig. 10, the band gap energy value is found to increase from 3.50 eV to 4.00 eV as a result of the increasing annealing temperature from 150 °C – 200 °C. The direct optical band gap energy of NiO-PbS thin films was reported to increase from 1.38 eV to 2.38 eV (Augustine *et al.*, 2018), which shows that our findings are comparable with others [29].

However, Augustine and Nnabuchi (2018) reported a decrease in the energy band gap of CuO-PbS thin films from 4.13 eV to 3.90 eV as a result of increase in annealing temperature from 200-400^{o}C which differs from our findings in terms of trend with annealing temperature but agrees with our findings in terms of magnitude and range of the band gap [23].

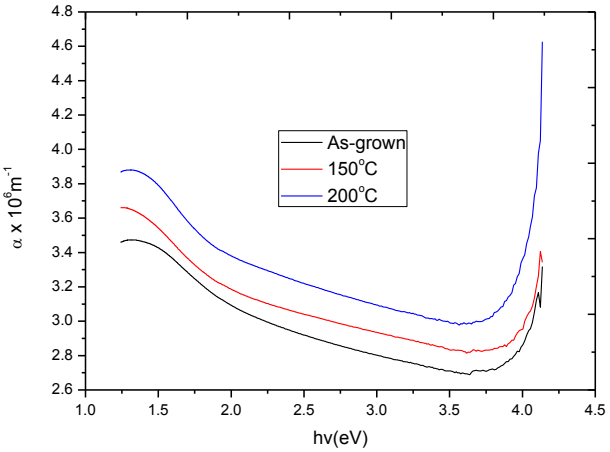

Fig. 9. Plots of α versus photon energy.

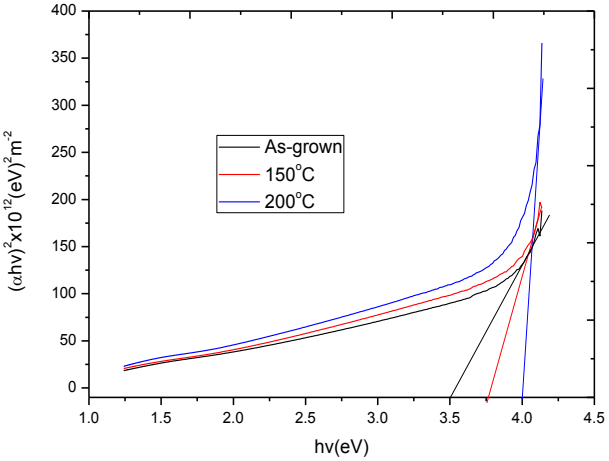

Fig. 10. Plots of $(\alpha hv)^2$ versus photon energy.

From Fig. 11, we can see that the extinction coefficient (k) showed similar behaviour of the corresponding absorption coefficient. This may be attributed to the linkage in the mathematical equations relating both parameters. It is also important to mention that extinction coefficient is the sum of absorption coefficient and scattering coefficient. Extinction coefficient decreases with increasing photon energy at 4 eV and then increases slightly. Extinction coefficient, k generally varies from 0.75 to 2.70 for as-grown, 0.80 to 2.85 for annealed at 150^{o}C and 0.85 to 3.00 for annealed at 200^{o}C. The extinction coefficient increases with annealing temperature with similar order of magnitude reported by other authors [23].

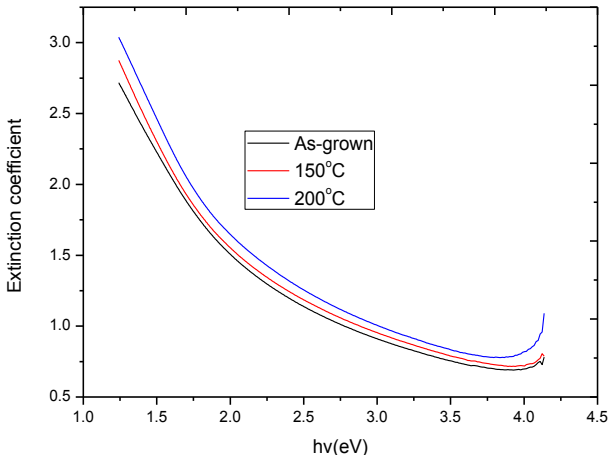

Fig. 11. Plots of extinction coefficient versus photon energy.

4. Conclusion

The synthesis of Cu_2O/PbS thin films using chemical bath deposition technique was successfully carried out. The structural, morphological and optical characterization of the films were carried out using x-ray diffractometer, scanning electron microscope and spectrophotometer respectively. The quantitative measurement of the elemental composition of the films was done using Rutherford backscattering technique. The scanning electron micrographs of the films depicted particles of different sizes scattered across the film surface. The optical parameters varied considerably with the parametric investigation involving post deposition temperature. In particular, the band gap energy exhibited a blue shift, increasing from 3.50eV to 4.00eV. The band gap are in the required intervals for use as window layers in the fabrication of solar cells.

References

[1] M. N. Nnabuchi, Journal of Research Science 17(4), 263 (2006)

[2] H. Tabor, Selective surfaces in solar energy conversion: An introduction course, In: A.E.Dixon and J. D. Leslie (Eds.), Selected Lectures From The 5th Course on Solar Energy Conversion, University of Waterloo, Ontario, Aug 6-19, 1979, Pergamon Press, Oxford, UK; https://doi.org/10.1016/B978-0-08-024744-1.50014-0

[3] B. Meinel, M. P. Meinel, Applied Solar Energy: An Introduction, Addison-Wesley and Co., Reading, UK (1979).

[4] P. N. Kalu, D. U. Onah, P. E. Agbo, C. Augustine, R. A. Chikwenze, F. N. C. Anyaegbunam, C. O. Dike, Journal of Ovonic Research 14, 293 (2018).

[5] R. A. Chikwenze, M. N. Nnabuchi, Chalcogenide Letters 7, 401 (2010).

[6] M. N. Nnabuchi, Pacific Journal of Science and Technology 6(2), 105 (2005).

[7] M. N. Nnabuchi, S. O. Onyishi, Proceedings of the 1st of the African International Conference/Workshop on Application of Nanotechnology to Energy, Health and Environment, UNN, March 23-29, 2014.

[8] M. N. Nnabuchi, Pacific Journal of Science and Technology 7(1), 69 (2006).

[9] K. A. Nnaemeka, E. Laz, N. S. Umeokwonna, Proceedings of the 1st African International Conference/Workshop on Applications of Nanotechnolgy to Energy, Health and Environment, March 23-29, (2014).

[10] O. Odezue, N. A. Okereke, K. L. Ezenwa, Proceedings of the 1st African International Conference/Workshop on Applications of Nanotechnolgy to Energy, Health and Environment, March 23-29 (2014).

[11] M. A. Manal, H. H. Noor, I. M. Hanaa, H. M. Ghuson, A. A. Kadhim, F. A. Ameer, Journal of Electron Devices 12, 761 (2012).

[12] A. A. El Meh, S. Ershov, N. Britun, A. Richard, S. Kunstantinidis, R. Synders, Spectrochimica Acta Part B, 99 (2015); https://doi.org/10.1016/j.sab.2014.11.009

[13] P. E. Agbo, M. N. Nnabuchi, D. U. Onah, Journal of Ovonic Research 7, 29 (2011).

[14] K. Ahmadi, A. A. Ziabari, K. Mirabbaszadeh, A. A. Shal, Bull. Mater. Sci. 38, 617 (2017); https://doi.org/10.1007/s12034-015-0898-8

[15] P. E. Agbo, M. N. Nnabuchi, Chalcogenide Letters 8, 273 (2011).

[16] P. E. Agbo, Chemistry and Materials Research 6, 42 (2014).

[17] P. E. Agbo, Advances in Applied Science Research 2, 393 (2011).

[18] S. O. Onyishi, M. N. Nnabuchi, C. Augustine, IOSR Journal of Applied Physics 19(5), 1 (2018).

[19] A. I. Onyia, M. N. Nnabuchi, Proceedings of the 1st African International Conferences/Workshop on Applications of Nanotechnology to Energy, Health and Environment, UNN, March 23-29 (2014).

[20] C. Augustine, M. N. Nnabuchi, F. N. C. Anyaegbunam, A. N. Nwachukwu, Digest Journal of Nanomaterials and Biostructures 12, 523 (2017).

[21] M. N. Nnabuchi, C. Augustine, Materials Research Express 5, 1 (2018); https://doi.org/10.1088/2053-1591/aab589

[22] C. Augustine, M. N. Nnabuchi, Materials Research Express 5, 1 (2018).

[23] C. Augustine, M. N. Nnabuchi, F. N. C. Anyaegbunam, C. U. Uwa, Chalcogenide Letters 14, 321 (2017).

[24] C. Augustine, M. N. Nnabuchi, Journal of Ovonic Research 13, 233 (2017).

[25] C. Augustine, M. N. Nnabuchi, Journal of Non-Oxide Glasses 9, 85 (2017).

[26] C. Augustine, M. N. Nnabuchi, P. E. Agbo, F. N. C. Anyaegbunam, R. A. Chikwenze,C. N. Nwosu, P. N. Kalu, U. Uba, R. O. Okoro, S. O. Onyishi, Journal of Ovonic Research 14, 339 (2018).

[27] C. Augustine, R. A. Chikwenze, F. N. C. Anyaegbunam, B. J. Robert, E. P. Obot, P. N. Kalu, Global Journal of Engineering Science and Researches 6(2), 249 (2019); https://doi.org/10.1088/2053-1591/ab1058

[28] C. Augustine, R. A. Chikwenze, F. N. C. Anyaegbunam, B. J. Robert, E. P. Obot, P. N. Kalu, Global Journal of Engineering Science and Researches 6(2), 267 (2019); https://doi.org/10.1088/2053-1591/ab1058

[29] C. Augustine, M. N. Nnabuchi, R. A. Chikwenze, F. N. C. Anyaegbunam, P. N. Kalu, B. J. Robert, C. N. Nwosu, C. O. Dike, E. N. Taddy, Mater. Res. Express, 6 (2019); https://doi.org/10.1088/2053-1591/ab1058